




# Facile construction of a degradable and renewable superhydrophobic indole-based hemiaminal aerogel for efficient oil–water separation

Rui Guo<sup>1</sup>, Yuyu Zhang<sup>1</sup>, Lun Wang<sup>1</sup>, Yin Huang<sup>1</sup>, Rui Yuan<sup>1</sup>, Li Yang<sup>1,\*</sup> , and Guanjin Chang<sup>1,\*</sup>

<sup>1</sup> State Key Laboratory of Environment-Friendly Energy Materials and School of Materials and Chemistry, School of Manufacturing Science and Engineering, Southwest University of Science and Technology, Mianyang 621010, People's Republic of China

**Received:** 29 March 2023

**Accepted:** 6 May 2023

**Published online:**  
17 May 2023

© The Author(s), under exclusive licence to Springer Science+Business Media, LLC, part of Springer Nature 2023

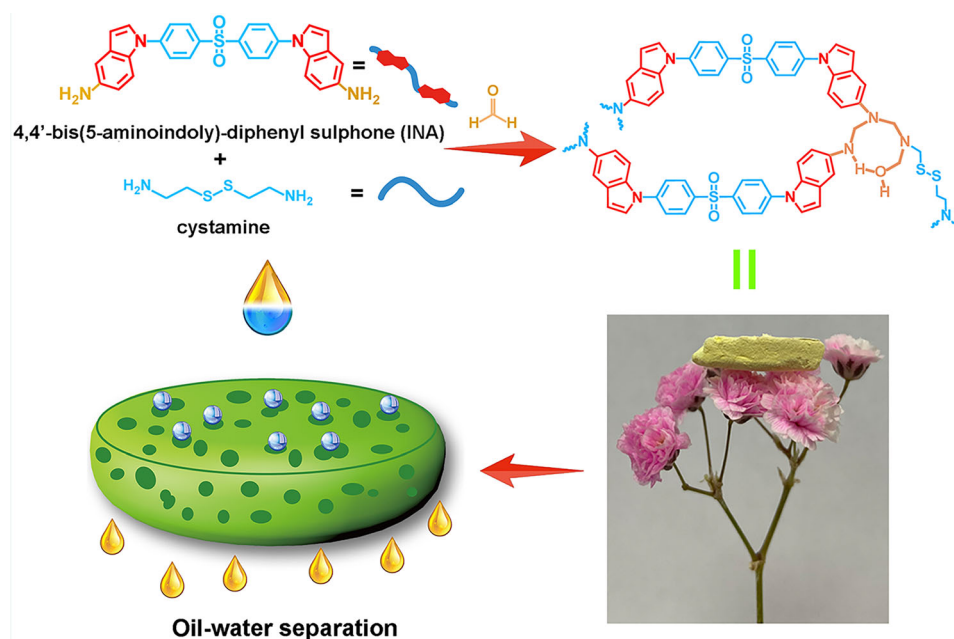
## ABSTRACT

Design readily available and inexpensive aerogels as potential sorbent materials for oil–water separation is extremely significant because of the increasing discharge of domestic oil pollution. Hereby, a novel superhydrophobic indole-based hemiaminal aerogel (PCINA) without any post-surface treatment was fabricated by a facile, simple and mild method via sol–gel technology followed by freeze-drying. The as-obtained indole-based hemiaminal aerogel exhibited high absorption capacity for varieties of oils and organic solvents. In addition, the separation efficiency of oil–water mixture was as high as 99.8%, even the separation efficiency of emulsion could achieve to 98.2%. More excitingly, the indole-based hemiaminal aerogel PCINA possessed repeatability and regeneration due to the feasible desorption and rapid degradation, suggesting that the green and renewable aerogel was a promising material for the treatment of oil contaminants in different fields.

Handling Editor: Maude Jimenez.

Address correspondence to E-mail: yanglichem628@126.com; gjchang@mail.ustc.edu.cn

## GRAPHICAL ABSTRACT



## Introduction

Nowadays, in view of extensive applications of oils and organic solvents in fuel, industry, energy source as well as chemical research, the rapid increase in industrial oily effluent in daily life and the frequent oil spill accidents have created a serious threat to the aquatic ecosystems and even human living environment [1–5]. Exxon Valdez oil spill (EVOS) happened in 1989 has brought fatal damage to nearly thousands of living species in the habitat and had disastrous consequences up to now [6]. Thus, it is a challenging task to effectively clean up oily wastewater. Conventional treatments including in situ burning [7], degradation [8, 9], sedimentation [10], skimming [11], and electrochemical technology [12, 13] can resolve the tickler of oil spill but are inefficient, time consuming, sophisticated, and apt to cause secondary pollution. As attractive alternatives, physical absorption and separation methods have been fueled and attracted widespread interest because of their convenience and relatively low cost [14, 15]. However, traditional absorbents such as inorganic zeolites

[16] and natural materials [17] reported in the literature faced serious drawbacks of low absorption capacity and relatively poor recyclability. Therefore, the exploration of readily accessible oil-absorbing materials with high efficiency and environment friendly continues to be an urgent ecological issue.

Over the past few decades, as one of the most promising candidates for the oil absorption, aerogels are an intriguing class of porous materials owing to their low densities, high porosities, high surface areas, excellent thermal and chemical stabilities, as well as their tunable surface chemistry [18–21]. To deal with the problem of oil–water mixture separation in recent years, a wide range of aerogel adsorbents have been designed and fabricated for oil collection and filtration [22–28]. Among the examples reported, the aerogel as an efficient oil sorbent usually needed a proper three-dimensional (3D) interconnected structure substrate and a special wettability surface. For instance, Ieamvitevanich et al. functionalized bacterial cellulose by coprecipitation of  $\text{Fe}_3\text{O}_4$  nanoparticles before pyrolysis to produce a magnetic carbon nanofiber aerogel and found it had hydrophobic/oleophilic properties [25].

Jiang and coworkers presented a gelatin/TiO<sub>2</sub>/polyethyleneimine composite aerogel, which had the 3D structure with the hierarchical porous structure and a superamphiphilic surface, endowing it with excellent oil–water separation properties [26]. Despite considerable effort, the availability of such aerogels with selective wettability surface was limited to a certain extent for some reasons, including the complicated synthetic route, the pyrolysis of aerogel or the demand of additional reagents for hydrophobic modification [22], and more cost and energy consuming. Accordingly, the development of facile aerogels without any post-surface treatment to high effectively absorb and separate oil from water is significant and necessary.

Emerging as a new type of functional and smart dynamic covalent materials, hemiaminal organogels can possess reversible behavior triggered by stimuli such as pH, redox conditions or temperature [29]. Although hemiaminal organogels materials have been extensively investigated and utilized in self-healing, printable materials, and adhesives [29], the design of hemiaminal aerogel as oil sorbents for high-efficiency oil–water separation especially emulsion separation has not been thoroughly explored [30]. Recently, we described a new crosslinking polyhexahydrotriazines with unprecedented toughening and recyclable properties based on the cation- $\pi$  interactions of indole ring and the sensitivity to pH of the hemiaminal moiety [31]. In particular, we reported a novel aminoindole-based smart aerogel could visually detect and efficiently remove of 2,4,6-trinitrotoluene in water with good reusability via the cation- $\pi$  interactions [32]. Enlightened by these studies and considering the hydrophobic of the disulfide bonds [33, 34], we hypothesized that introduction of the cystamine to the hemiaminal aerogel would facilitate the superhydrophobic property and enhance the oil selective absorption process.

In this work, we postulated a facile, mild and easily controllable condensation technique for the synthesis of a novel indole-based hemiaminal aerogel (PCINA) via sol–gel technology followed by freeze-drying (Fig. 1). Series of characterizations and tests, including the aerogel structure, wettability, oil absorption and desorption, as well as oil–water separation efficiency, have been studied in detail. As anticipated, the indole-based hemiaminal aerogel PCINA

possessed a 3D porous structure, good superhydrophobic property without any post-surface treatment, selective oil uptake capacity, and high effective oil–water mixture separation. More interestingly, the indole-based hemiaminal aerogel after use could be rapidly degradable and the raw material was able to recover for recycling through the simple approaches, ensuring material sustainability and avoiding the secondary pollution to environment. These results suggested that the indole-based hemiaminal aerogel as oil absorbent was an attractive candidate for oil–water separation owing to its green, readily available and renewable property. Furthermore, these studies will help us to gain a deeper insight into the absorption and desorption mechanism in oil–water separating process and enrich works in treating oil contaminants or removing pollutants from aqueous environments by the aerogels.

## Experimental

### Materials and measurements

5-Nitroindole, bis(4-fluorophenyl) sulfone, cystamine dihydrochloride, formaldehyde aqueous (HCHO, 37%), and Pd/C (5 wt%) were purchased from Aladdin Reagent (Shanghai) Co., Ltd. and without further purification. The rest of the materials and reagents were obtained from different commercial sources and used without further purification.

Fourier-transform infrared spectroscopy (FT-IR) was recorded on Nicolet-6700 FT-IR spectrometer. <sup>1</sup>H NMR and <sup>13</sup>C NMR spectra were performed on a Bruker 400 MHz NMR spectrometer with CDCl<sub>3</sub> as the internal standard. Solid-state cross-polarization magic-angle-spinning (CP/MAS) NMR spectrum was performed on a Bruker Avance III 400 NMR spectrometer. The scanning electron microscopy (SEM) image was conducted on an S-4800 (Hitachi Ltd.) field emission scanning electron microscope system. Digital photographs were taken using a Cannon 600D camera. The pH values were accurately determined by using a pH meter (pHS-3E). Water contact angles (WCAs) were made on a Sindin SDC-350 machine. The static water CA images were captured after placing a 5  $\mu$ L droplet onto the surface.

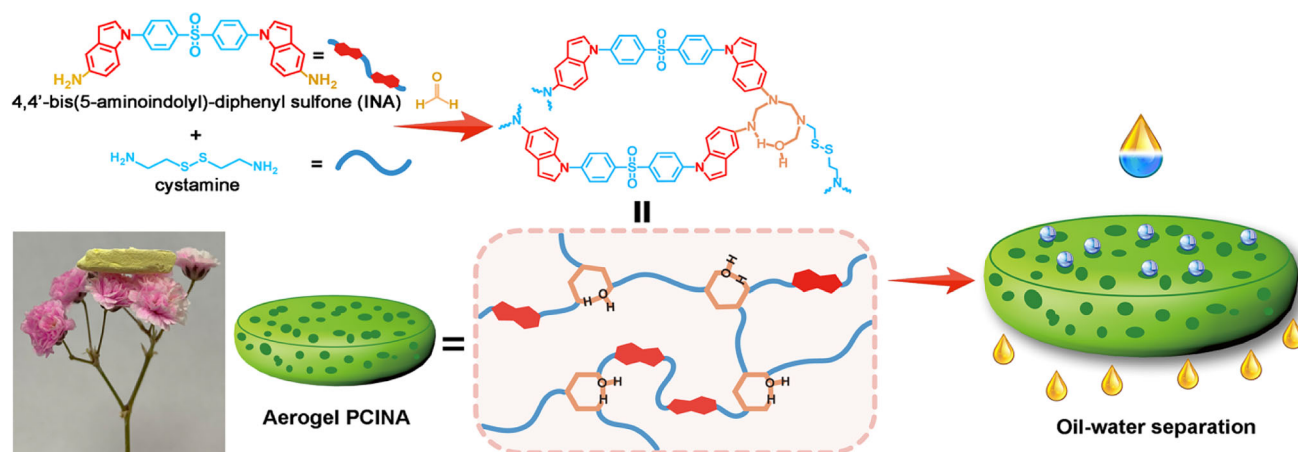


**Figure 1** Fabrication of the aerogel PCINA and a schematic illustration of PCINA for oil–water separation.

## Preparation of indole-based hemiaminal polymer aerogel

### Synthesis of cystamine

In an Erlenmeyer flask, cystamine dihydrochloride (8.00 g, 35.5 mmol) was dissolved in 100 mL distilled water. Potassium hydroxide (6.00 g, 107 mmol, 1.5 eq to HCl) was added and the mixture was stirred for 10 min. The resulting mixture was extracted with  $4 \times 150$  mL  $\text{CH}_2\text{Cl}_2$ , the combined organics were dried over  $\text{MgSO}_4$ , filtered, and solvent was removed to yield a colorless to slightly yellow oil (4.3 g, 80%).  $^1\text{H}$  NMR (400 MHz,  $\text{CDCl}_3$ )  $\delta$  = 1.46 (s, 2H), 2.77 (t, 2H), 3.02 (t, 2H) ppm;  $^{13}\text{C}$  NMR (100 MHz,  $\text{CDCl}_3$ )  $\delta$  = 40.5, 42.4 ppm.

### Synthesis of 4,4'-bis(5-nitroindolyl)-diphenyl sulfone (INN)

A two-necked flask (25 mL) was equipped with a magnetic stirrer, a rubber septum, and a water-cooled condenser. The reaction vessel was evacuated and back-filled with nitrogen and this sequence was repeated three times. Bis(4-fluorophenyl) sulfone (0.509 g, 2.00 mmol), 5-nitroindole (0.811 g, 5.00 mmol),  $\text{K}_2\text{CO}_3$  (0.691 g, 5.00 mmol), and NMP (8.0 mL) were added successively under a stream of nitrogen at room temperature. The reaction mixture was heated to 180 °C under stirring for 4 h. The resulting solution was allowed to slowly cool to room temperature, and subsequently poured into cold water, filtered, washed with water. The crude product was purified by silica gel column

chromatography using dichloromethane as an eluent to afford INN as a yellow crystal (yield 96%). FT-IR spectrum (KBr pellet,  $\text{cm}^{-1}$ ): 3452, 3104, 1590, 1515, 1328, 1150, 764, 741, 613;  $^1\text{H}$  NMR (400 MHz,  $\text{CDCl}_3$ ):  $\delta$  = 6.93 (d,  $J$  = 3.4 Hz, 1H), 7.49 (d,  $J$  = 6.5 Hz, 2H), 7.59 (d,  $J$  = 9.2 Hz, 1H), 7.72 (d,  $J$  = 5.4 Hz, 1H), 8.16 (d,  $J$  = 9.1 Hz, 1H), 8.23 (d,  $J$  = 8.6 Hz, 1H), 8.65 (d,  $J$  = 2.2 Hz, 1H) ppm;  $^{13}\text{C}$  NMR (100 MHz,  $\text{CDCl}_3$ ):  $\delta$  = 106.5, 109.6, 117.7, 117.8, 123.9, 128.3, 129.1, 129.6, 137.3, 139.0, 141.9, 142.1 ppm.

### Synthesis of 4,4'-bis(5-aminoindolyl)-diphenyl sulfone (INA)

To a two-necked flask (25 mL) equipped with a magnetic stirrer, a nitrogen outlet, inlet, and a water-cooled condenser, INN (538 mg, 1.00 mmol) and Pd/C (54.0 mg, 10 wt% of INN) were dissolved in 1,4-dioxane (2 mL), and then hydrazine hydrate (50  $\mu\text{L}$ ) was slowly added into the solution. The reaction mixture was heated to 100 °C, with stirring until all of INN was reduced to INA (determine the degree of reaction based on the thin layer chromatography). The resulting solution was allowed to slowly cool to room temperature, and subsequently poured into cold water, filtered to remove the unreacted hydrazine hydrate. The residue was dissolved in ethyl acetate and removed the Pd/C by filtering. After the solvent was evaporated, the solid was purified by column chromatography (ethyl acetate: petroleum ether = 2:1) which afforded a light yellow solid (yield 80%). FT-IR spectrum (KBr pellet,  $\text{cm}^{-1}$ ): 3440, 3360, 2940, 1730, 1660, 1510, 1460, 1300, 1180, 760, 620;  $^1\text{H}$  NMR (400 MHz,  $\text{CDCl}_3$ ):  $\delta$  = 3.60 (s, 2H), 6.55 (d,

$J = 3.3$  Hz, 1H), 6.70 (d,  $J = 8.8$  Hz, 1H), 6.96 (d,  $J = 2.7$  Hz, 1H), 7.44 (d,  $J = 8.7$  Hz, 1H), 7.64 (d,  $J = 8.9$  Hz, 1H), 8.10 (d,  $J = 8.9$  Hz, 1H) ppm;  $^{13}\text{C}$  NMR (100 MHz,  $\text{CDCl}_3$ ):  $\delta = 105.0, 106.1, 110.1, 111.2, 113.5, 118.8, 123.3, 127.5, 129.5, 141.0, 144.3$  ppm.

### Preparation of hemiaminal aerogel PCINA

INA (246 mg, 0.500 mmol) and cystamine (76.4 mg, 0.500 mmol) was dissolved in N-methylpyrrolidone (NMP) (2 mL). The total solid content in the pre-gel solution was kept at 20 wt%. Subsequently, HCHO aqueous (168  $\mu\text{L}$ ) were added to the mixture and stirred for 3 h. The obtained solution aged at room temperature for 2 h, freeze-dried in the refrigerator for 5 h. The PCINA wet gel was washed with acetone and deionized water for 3 days to ensure that any residue raw materials were removed. The final dried aerogel PCINA was obtained by freeze-drying. It had the ability to withstand more than 100 times and 500 times its own weight and recovered completely without significant permanent deformation (Fig. S1).

### Absorption of various oils and organic solvents

Series of testing liquids including dimethyl silicone oil, rapeseed oil, gasoline, sesame oil, chili oil, vacuum pump oil, chloroform, dichloromethane, petroleum ether, hexane, toluene and ethyl acetate were used to evaluate the absorption capacity of PCINA. In a typical test, PCINA was soaked into the liquids. Then, it was taken out until it was saturated absorption. The oil uptake capacity  $K$  (g/g) of PCINA was determined as:

$$K(\text{g/g}) = (M - M_0) / M_0 \quad (1)$$

where  $M$  and  $M_0$  are the weights of PCINA before and after oil absorption, respectively. Each absorption test was repeated three times.

### Oil-water separation performance

The separation performance was tested using a mixture of oil and water (1:1, w/w). After absorption, the separation efficiency ( $R$ ) was evaluated as:

$$R(\%) = (M_r / M_0) \times 100\% \quad (2)$$

where  $M_r$  and  $M_0$  are the weights of the retained oil and the original oil in the mixture, respectively.

## Results and discussion

### Characterizations of PCINA

FT-IR and  $^{13}\text{C}$  CP/MAS NMR spectra were used to confirm the successfully prepared PCINA, and the results were in good agreement with the proposed structure (Fig. 2a and b). In the FT-IR spectrum of PCINA (Fig. 2a), the broad absorption peak at  $3444\text{ cm}^{-1}$  was attributed to the stretching vibration of N–H. The peaks at  $2932\text{ cm}^{-1}$  and  $2853\text{ cm}^{-1}$  were due to the stretching vibration of  $-\text{CH}_2-$  in the hemiaminal polymer network and the peaks at  $1675\text{ cm}^{-1}$  and  $1453\text{ cm}^{-1}$  were assigned to the vibrations of the aromatic ring skeleton. The stretching vibration peak of the tertiary amine C–N appeared at  $1160\text{ cm}^{-1}$ . Moreover, the broad peaks in the NMR spectrum at 150–100 ppm were ascribed to all of the aromatic ring carbons, and the small resonance peaks located at 85–45 ppm was belonged to the methylene carbons of the hemiaminal ring. The peak at 30 ppm corresponded to the methylene carbons (Fig. 2b).

The obtained aerogel PCINA had a 3D network framework (Fig. 2c). The oval nanoparticles aggregated, interconnected, and further fused unprecedentedly to evolve into the extended multilevel mountain-like superstructures. The cystamine could enhance the hydrophobicity for the aerogel and these mountain-like nanostructures of PCINA successfully formed the very rough structures (Fig. 2d). It can be clearly seen that PCINA had a well-connected 3D porous structure and oil could easily flow through the aerogel with these abundant micropores on PCINA. Therefore, PCINA became hydrophobic with a WCA of  $150.3^\circ$ , which could not be made to wet and infiltrated by a water droplet.

In addition, XRD and XPS were used to confirm the successfully prepared PCINA, and the results were similar with the reported literature [35] (Fig. 3a–c). In the XRD of PCINA (Fig. 3a), the broad diffraction between  $10^\circ$  and  $30^\circ$  is observed originating from the scattering of hemiaminal structure, indicating its amorphous structure. Moreover, the X-ray photoelectron spectroscopy (XPS) was performed to study the detailed structural characteristics of PCINA. N and O are detected in survey spectra of PCINA. Figure 3b shows the N 1s XPS spectrum of PCINA, two peaks can be observed at 399.2 eV and 400.1 eV, corresponding to  $\text{sp}^2$  hybridized C–NH and  $\text{sp}^2$

**Figure 2** **a** FT-IR spectrum. **b**  $^{13}\text{C}$  CP/MAS NMR spectrum. **c** SEM images of prepared aerogel PCINA and with high magnification. **d** Inset: the image of the WCA of PCINA.

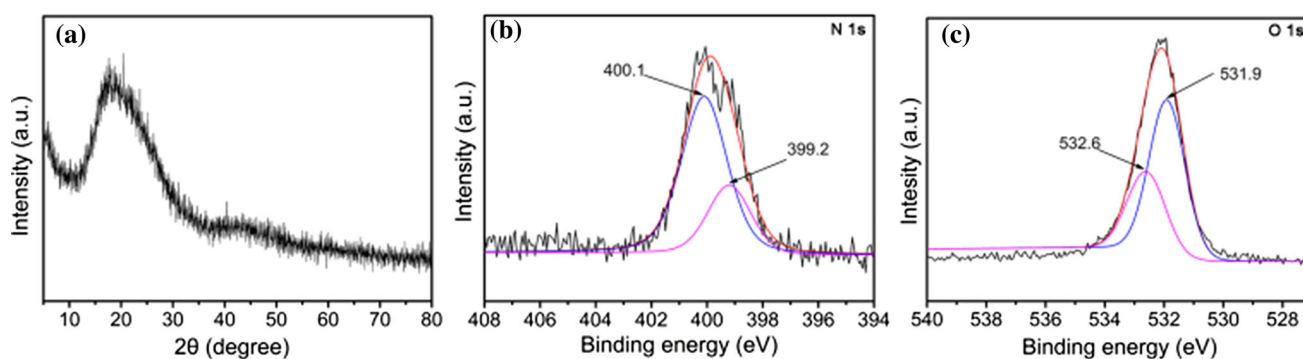
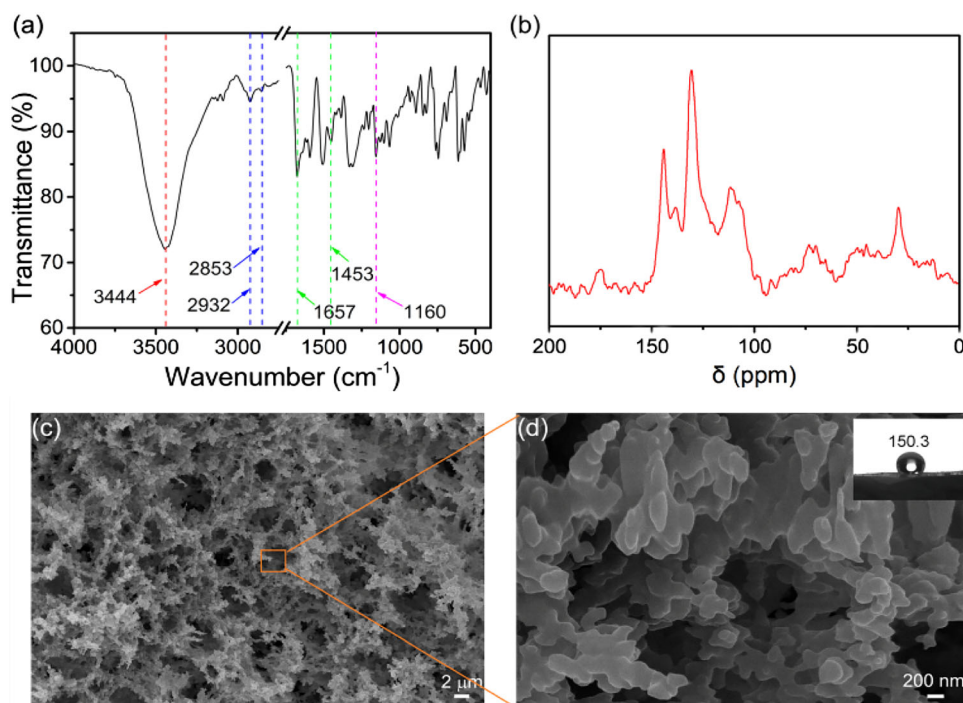


**Figure 3** **a** XRD spectra of the PCINA. **b** N 1s XPS spectrum of PCINA. **c** O 1s XPS spectrum of PCINA.

hybridized aromatic N in the indole (C–N–C), respectively. The spectrum of PCINA (Fig. 3c) exhibits two O 1s peaks at 531.9 and 532.6 eV, which are related to the O=S=O and the C–OH, respectively.

### Wetting properties of PCINA

Figure 4a exhibits that a water droplet formed a sphere on the surface of PCINA with a contact angle of  $150.3^\circ$ , after keeping in ambient air for 30 min, negligible changes in the WCA of the aerogel was observed. As mentioned above, PCINA showed superhydrophobic. The phenomenon of water droplets and silicone oil droplets on the aerogel PCINA was looked into to further prove the unique wetting properties. As depicted in Fig. 4b, when a methylene

blue-dyed water droplet was placed on the surface, PCINA repelled the water to make it take on an almost perfect sphere on the surface because of its low surface energy [36]. It was worth noting that the water droplets could slide off along with the sloping PCINA (Fig. 4c). Whereas, as soon as a Sudan III-dyed oil droplet contacted the PCINA surface, it immediately spread out and permeated through making the aerogel wet (Fig. 4d). Furthermore, PCINA also demonstrated stable and superhydrophobicity toward many corrosive solutions. It can be seen from Fig. 4e that PCINA also showed excellent hydrophobicity at pH 1–14. The WCAs of PCINA were all exceeded  $148^\circ$ . More importantly, the aerogel PCINA displayed good chemical resistance. In the

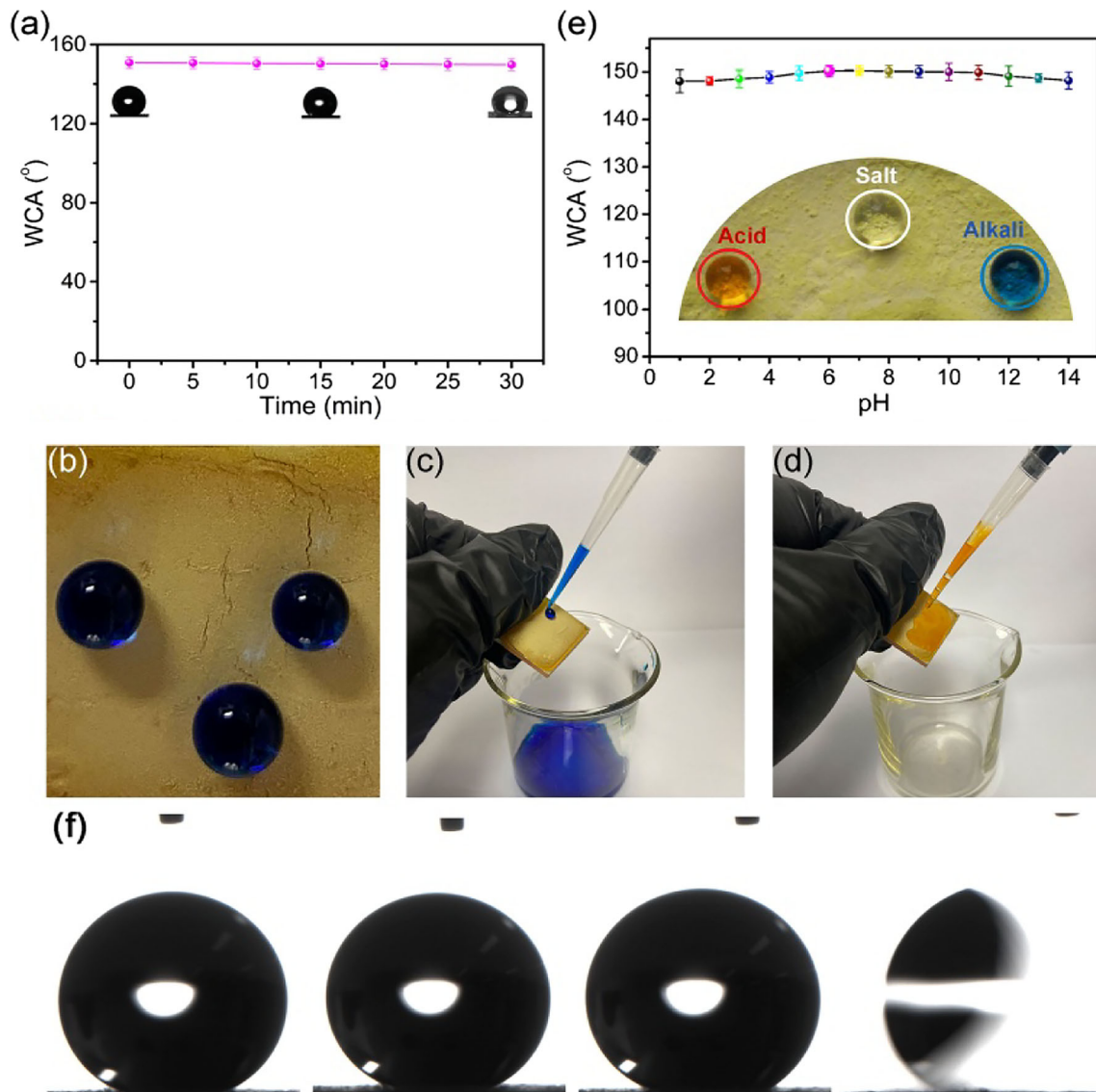


**Figure 4** **a** Variation in WCAs of PCINA upon exposure to air. **b** Still water droplets (dyed with methylene blue) on PCINA. **c** A stream of water sliding off along with the aerogel PCINA. **d** A stream of oil droplets (dyed with Sudan III-dyed) spreading out

inset of Fig. 4e, three different kinds of droplets (acidic, basic, and salt liquids) all maintained their spherical shapes. The sliding angle of PCINA is  $9.6^\circ$  as shown in Fig. 4f.

### Absorption of various oils and organic solvents

Owing to the 3D porous structure and superhydrophobicity of the hemiaminal aerogel, PCINA became an excellent oil absorbent candidate for oil-water separation. The adsorption capacities of

and seeping into the PCINA. **e** WCAs of PCINA at different pH values (inset displays the droplet of 1 M HCl, 1 M NaCl, and 1 M NaOH on the aerogel surface, respectively). **f** Sliding angle of PCINA.

PCINA were estimated by a variety of oils and organics, such as dimethyl silicone oil, rapeseed oil, gasoline, sesame oil, chili oil, vacuum pump oil, chloroform, dichloromethane, petroleum ether, hexane, toluene and ethyl acetate. Here, we chose a silicone oil/water mixture and a chloroform/water mixture as the typical light and heavy oil absorption models, respectively, to present our results. As shown in Fig. 5, when PCINA was soaked into the silicone oil/water mixture, the light Sudan III-dyed oil layer was gradually absorbed by the aerogel within a few minutes (Fig. 5a). As a contrast, PCINA

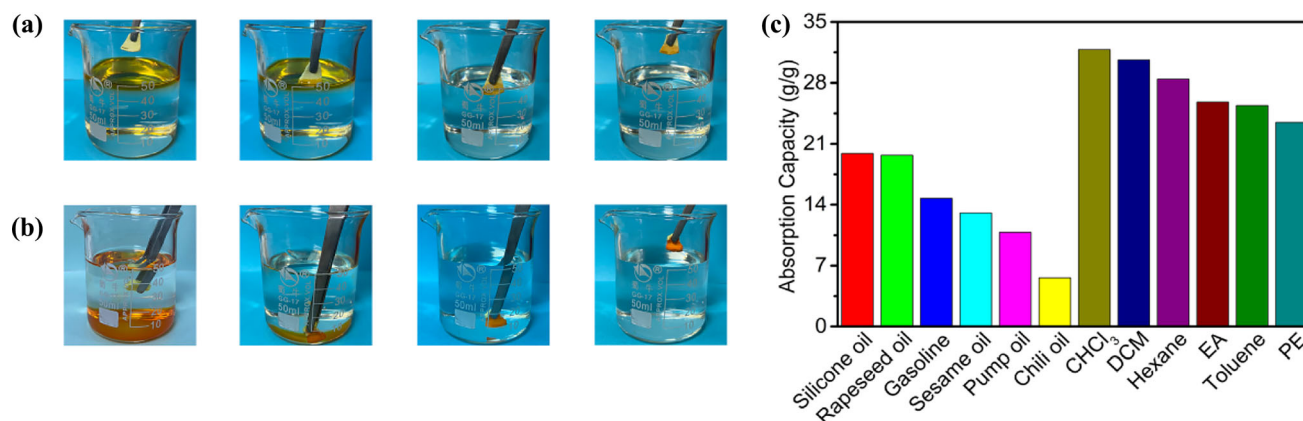


**Figure 5** Photographs of the absorption process of (a) light oil (silicone oil) floating on water and (b) heavy oil (chloroform) under water by PCINA. c Absorption capacities of PCINA toward different oils and organic solvents.

needed to capture the heavy oil chloroform (dyed with Sudan III) underwater (Fig. 5b). Interestingly, we found that the uptake of all chloroform on PCINA was much quicker than that of silicone oil. It was assumed that the chloroform was less viscosity due to the smaller molecules and more likely to enter the pores of the aerogel [37]. These results suggested that PCINA had special absorption selectivity toward oil and water and it could be a potential material for the removal of oil spills.

Subsequently, the loading capacity of PCINA for other kinds of oils and organics with different viscosity was evaluated. As indicated in Fig. 5c, PCINA had saturation absorption capacity with 31.81, 30.63, 28.42, 23.48, 25.42, 25.81, 19.90, 19.69, 14.73, 13.04, 5.60, and 10.85  $\text{g g}^{-1}$  for chloroform, dichloromethane, hexane, petroleum ether, toluene, ethyl acetate, dimethyl silicone oil, rapeseed oil, gasoline, sesame oil, chili oil, and vacuum pump oil, respectively. We inferred that the difference in absorption capacities of various oils and organic solvents was

ascribed to their different densities [37]. It was noted that the oil uptake ability of PCINA was comparable to other reported adsorbents [22, 37–42], for which the absorption capacities of various adsorbents are displayed in Table 1. The great adsorption capacity is attributable to the multi-aperture structure and low surface energy of PCINA [43]. As expected, these characteristics made PCINA a promising and competitive candidate for the treatment of oil pollution.

### Desorption and recyclability

For the desorption study, the oil loaded on PCINA could be removed in the sodium hydroxide aqueous solution with the pH value of 13.0. Despite the hydrophobicity of PCINA in basic solution, the oils dyed with Sudan III were still desorbed from the floating PCINA (Fig. S1). The reversibility of the extraction process was conducted ten times. It was found that the samples that were subjected to multiple recycling treatments also showed almost the

**Table 1** Comparison of absorption capacity ( $\text{g/g}^{-1}$ ) of various adsorbent materials

Absorbents materials	Adsorbates	Adsorption capacity ( $\text{g g}^{-1}$ )	References
SA/GO/SiO <sub>2</sub> -M aerogel	Hexane, chloroform, CCl <sub>4</sub> , etc.	17.92–43.92	[20]
Cellulose sponge	Chloroform	7.0	[32]
Polypyrrole nanotubes	Hexane	8.0	[33]
Amphiphobic polyHIPEs	Hexadecane	20.9	[34]
Silane functionalized PVA formaldehyde sponges	DCM, CCl <sub>4</sub> , coleseed oil, etc.	4.0–14.0	[35]
Modified polylactic acid nonwoven fabrics	Hexane, CCl <sub>4</sub>	~ 4.0, ~ 6.0	[36]
CNFs based PDMS foam	Silicone oil, chloroform, etc.	1.4–8.6	[37]
Indoled-based hemiaminal aerogel PCINA	Silicone oil, chloroform, etc.	19.90–31.81	This work



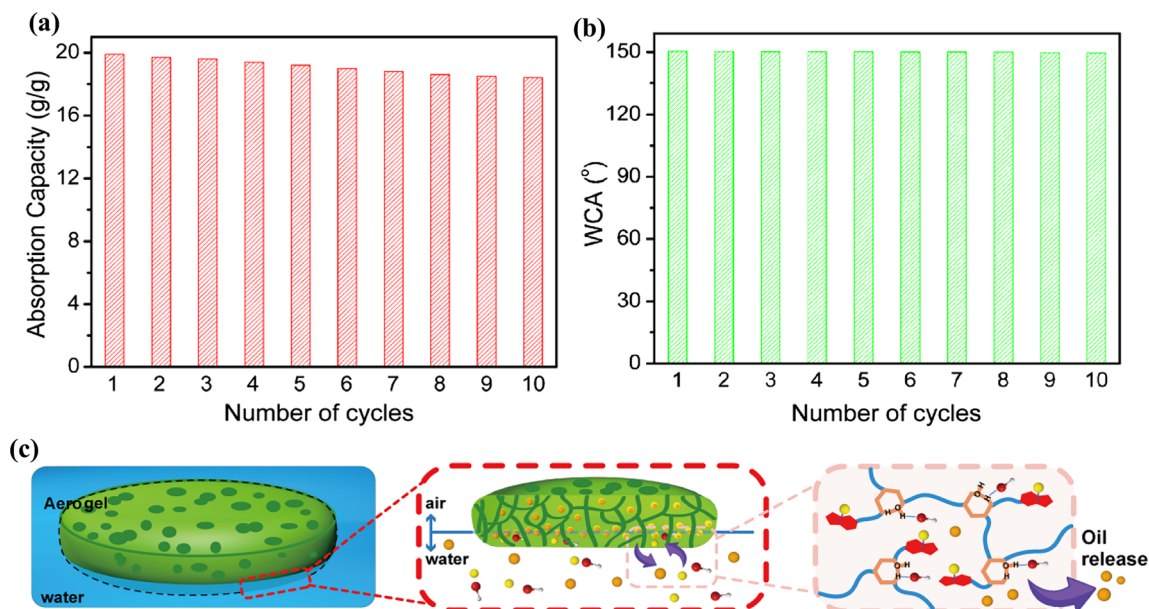


**Figure 6** **a** Absorption recyclability of PCINA for silicone oil. **b** Water contact angle of PCINA over ten successive recycling processes. **c** A schematic representation of the desorption mechanism by which the aerogel PCINA uptake of oil can

slowly release the oil in water with pH at 13.0 (color code: oil, orange;  $\text{Na}^+$ , yellow;  $\text{OH}^-$ , red; blue dash lines mean the cation- $\pi$  interaction between  $\text{Na}^+$  and indole ring or hydrogen bonding between  $\text{OH}^-$  and the hemiaminal structure).

same absorption behavior as the original material and the capacity was maintained to  $18.4 \text{ g g}^{-1}$  (Fig. 6a), revealing the indole-based hemiaminal aerogel could be reused. At the same time, the water contact angle of PCINA was measured after each recycling process. Even after 10 recycling processes, the WCA remained larger than  $149.5^\circ$  (Fig. 6b), indicating that the aerogel was superhydrophobic yet. To gain a more comprehensive understanding on the oil desorption mechanism of the PCINA in NaOH solution, an illustration of the desorption process is exhibited in Fig. 6c. We speculated that the reasons for desorption were the competition interactions between water and oil molecules with PCINA. The indole ring of PCINA was available for  $\text{Na}^+$  binding via the well-known cation- $\pi$  interactions [44], besides, the hydroxide ions in the basic solution would interact with the hemiaminal structure of PCINA through hydrogen bonding. Consequently, these synergistic effects were stronger than the van der Waals force between the oils and PCINA, giving rise to the oils were resisted from the pores and released into the solution (Fig. 6c).

### Degradation and regeneration

To our best knowledge, avoiding secondary pollution during oil–water separation and developing the renewable process of the absorbent material are very significant for energy conservation and environmental protection. More gratifyingly, herein, the reversible formation and degradation of the hemiaminal

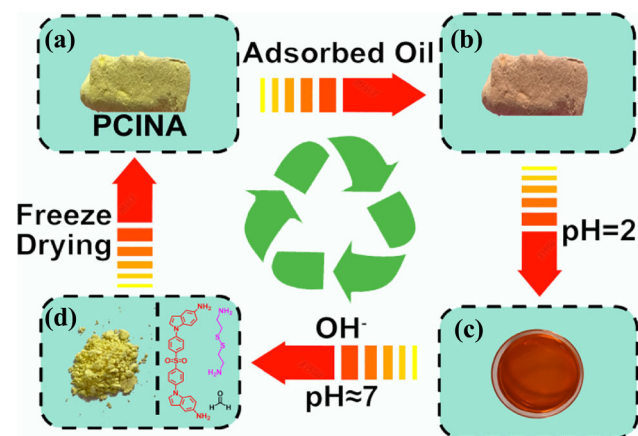


**Figure 7** Diagram of a recycling process from waste to a new aerogel: **a** An optical image of PCINA; **b** The PCINA adsorbing oil from water (oil dyed with Sudan III); **c** The PCINA was hydrolyzed in sulfuric acid solution (pH = 2.0); **d** After neutralizing, the monomers powder of PCINA was recovered.

cyclic structure through the adjustment of pH enabled PCINA to be regenerated feasibly and easily (Fig. 7). For example, by adding a certain amount of sulfuric acid solution and keeping the pH at 2.0, PCINA quickly collapsed and was split into little pieces even after absorbing silicone oil from the oil–water mixture. Next, the little pieces further hydrolyzed and totally became the monomers dissolved into acid solution within ten minutes (Fig. 7c). Moreover, the monomers were successfully recovered by upon addition of saturated  $\text{Na}_2\text{CO}_3$  solution to neutralize the acid solution (Fig. 7d). Then, the recyclable monomers can be transformed into the aerogel after undergoing the freeze-drying process again (Fig. 7a). These results demonstrated that the tremendous potential of PCINA for infinite recycling and there were no secondary pollution problems to the environments. Compared with the superhydrophobic functional membrane separated from oil and water [45, 46], its degradation ability and regeneration ability were not inferior.

### Oil–water separation

To evaluate the practical application of the aerogel PCINA, oil–water separation experiments under gravity were performed using a mixture of Sudan-III-dyed oil and water (1:1, V/V) as model wastewater. Polypropylene syringe filters (0.45 mm) equipped with a piece of PCINA aerogel and syringe (5 mL) were used as the filtering apparatus (Fig. 8). A mixture of hexane (dyed by Sudan-III) and water was poured into the syringe. It was clearly found that the red silicone oil quickly permeated the hydrophobic aerogel under gravitational force, while the water was retained above the aerogel (Fig. 8a). In addition,

PCINA could also separate the gasoline/water mixture (Fig. 8b). The results proved that the 3D porous structures of PCINA might have advantageous effects on the filtration and the special wettability might enhance the interception and coalescence of water droplets [22]. As displayed in Fig. 8d, the separation efficiency ( $R$ ) for two types of oils decreases still remained around 98.0% after several cycles despite some slight fluctuations in the process, showing a good separation effect.

In real life, oil–water mixtures, which need to be treated, are somehow without obvious interfaces, such as emulsions. As we know, efficient emulsion separation in an eco-friendly, effective, and economical manner is still a great challenge. In this work, we also investigated the oil–water separation performance on emulsions. Span-80 (50  $\mu\text{L}$ ) was added into a 0.5 g mixed solution of gasoline and water to form an emulsion. The separation efficiencies of the emulsion of gasoline–water with mass ratios of 99:1, 9:1, 8:2, and 7:3 were 98.2, 98.1, 78.8 and 68.9%, respectively (Fig. 8e). Compared with other materials on the emulsion separation efficiency, the separation efficiency of PCINA ( $V_{\text{gas}}:V_{\text{water}} = 9:1$ , 98.1%) was no less than that of other materials, such as the PASP/PAA/PVA PFOTES filter cloth ( $V_{\text{oil}}:V_{\text{water}} = 9:1$ , 79.9%) [47], and a wood slice covered by copper hydroxide ( $V_{\text{oil}}:V_{\text{water}} = 50:1$ , > 98%) [48]. All testing results showed that the separation ability was gradually decreased as the amount of the emulsion increased, which was ascribed to that the surface of the aerogel might be polluted by surfactants [22]. We expect the PCINA aerogel was qualified for practical application in the efficient treatment of oil spill.

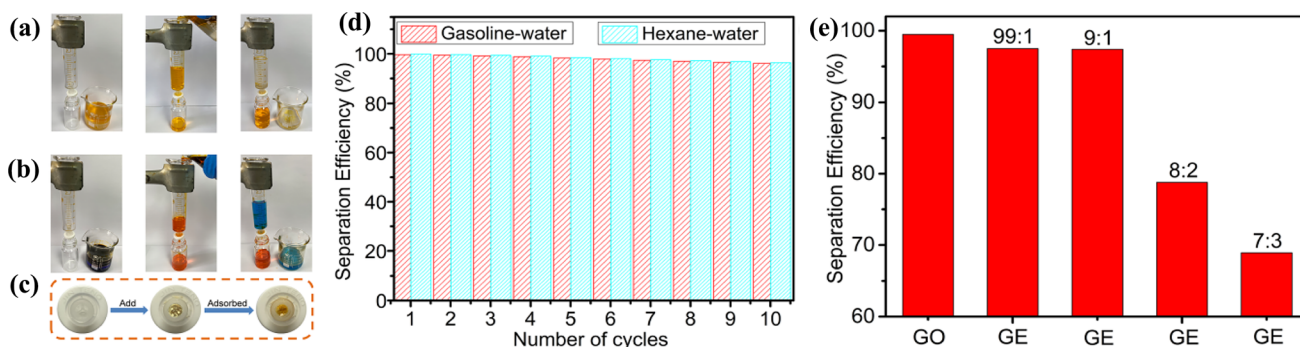


**Figure 8** a Controllable hexane/water separation using PCINA. b Controllable gasoline/water separation using PCINA. c Diagram of PCINA as the filter. d The separation efficiencies

of hexane/water and gasoline/water. e The separation efficiency of gasoline (GO) and gasoline/water emulsions (GE).

## Conclusions

In summary, we have proposed a facile and mild method to successfully prepare a superhydrophobic indole-based hemiaminal aerogel PCINA without any post-surface treatment, endowing it with selectivity for oil adsorption from water. Taking advantage of the 3D porous structure, an excellent oil absorption capacity and high efficiency of oil–water mixture separation especial emulsion separation could be obtained as expected. Moreover, the PCINA aerogel displayed good repeatability through desorption of oil in basic solution via the competition hydrogen bonding and cation- $\pi$  interactions. More importantly, the indole-based hemiaminal aerogel after use could be rapidly degradable and the raw material was able to recover for regeneration, which meant that the aerogel is green and environmentally friendly. Therefore, we believed that the obtained “oil-removing” type aerogel had great prospects in practical oil pollution treatments such as oil spill cleanup, fuel purification, and emulsion separation. This work may also greatly aid the design and construction of new advanced materials for the resolving the oily wastewater problems.

## Acknowledgements

This work was financially supported by the National Natural Science Foundation of China (21973076 and 22006122), the Project of the Central-Guided Local Science and Technology Development (2022ZYD0025), the Sichuan Talent Fund for Distinguished Young Scholars (2021JDJQ0033), the Applied Basic Research Programs of Sichuan Science and Technology Department (2021YJ0059), the Natural Science Foundation of Sichuan Province (2022NSFSC0310), and the Innovation and Development Fund of China Academy of Engineering Physics (CX20210039).

## Author contribution

RG and YZ performed the characterization analysis and application experiments. RG and RY synthesized the samples. YH and GC conceived the study. RG, LY, LW and GC wrote the manuscript.

## Data availability

Some or all data that support the findings of this study are available from the corresponding author upon reasonable request.

## Declarations

**Conflict of interest** There are no conflicts to declare.

**Ethical approval** Not applicable.

**Supplementary Information:** The online version contains supplementary material available at <http://doi.org/10.1007/s10853-023-08564-7>.

## References

- [1] Chang J, Ong C, Shi Y, Yuan J, Ahmed Z, Wang P (2021) Smart sand by surface engineering: toward controllable oil/water separation. *Ind Eng Chem Res* 60:9475–9481. <https://doi.org/10.1021/acs.iecr.1c01450>
- [2] Liu C, Peng Y, Huang C, Ning Y, Shang J, Li Y (2022) Bioinspired superhydrophobic/superhydrophilic janus copper foam for on-demand oil/water separation. *ACS Appl Mater Interfaces* 14:11981–11988. <https://doi.org/10.1021/ac sami.2c00585>
- [3] Bai Z, Jia K, Liu C et al (2021) A solvent regulated hydrogen bond crosslinking strategy to prepare robust hydrogel paint for oil/water separation. *Adv Funct Mater* 31:2104701. <https://doi.org/10.1002/adfm.202104701>
- [4] Huang J, Lu Z, Li J, Jia F, Wang Y, Hua L (2023) In situ growth of ZIF-8 onto aramid nanofiber composite aerogel for efficient removal of pollutants in water. *ACS Appl Polym Mater* 5:1606–1612. <https://doi.org/10.1021/acsapm.2c02110>
- [5] Li H, Yang H, Shu Y, Li C, Li B, Xiao W, Liao X (2023) Stainless steel screen modified with renatured xerogel for efficient and highly stable oil/water separation via gravity. *Langmuir* 39:3131–3141. <https://doi.org/10.1021/acs.langmuir.2c03307>
- [6] Grigorenko AN, Roberts NW, Dickinson MR, Zhang Y (2008) Nanometric optical tweezers based on nanostructured substrates. *Nat Photonics* 2:365–370. <https://doi.org/10.1038/nphoton.2008.78>
- [7] Lin Q, Mendelssohn IA, Bryner NP, Walton WD (2005) In-situ burning of oil in coastal marshes. 1. Vegetation recovery and soil temperature as a function of water depth, oil type, and marsh type. *Environ Sci Technol* 39:1848–1854. <http://doi.org/10.1021/es049063y>

- [8] Hazen TC, Dubinsky EA, DeSantis TZ et al (2010) Deep-sea oil plume enriches indigenous oil-degrading bacteria. *Science* 330:204–208. <https://doi.org/10.1126/science.1195979>
- [9] Prince RC (2015) Oil spill dispersants: boon or bane? *Environ Sci Technol* 49:6376–6384. <https://doi.org/10.1021/acs.est.5b00961>
- [10] Li L, Zhang J, Wang A (2018) Removal of organic pollutants from water using superwetting materials. *Chem Rec* 18:118–136. <https://doi.org/10.1002/tcr.201700029>
- [11] Broje V, Keller AA (2006) Improved mechanical oil spill recovery using an optimized geometry for the skimmer surface. *Environ Sci Technol* 40:7914–7918. <https://doi.org/10.1021/es061842m>
- [12] Li R, Rao L, Zhang J et al (2021) Novel in-situ electroflotation driven by hydrogen evolution reaction (HER) with polypyrrole (PPy)-Ni-modified fabric membrane for efficient oil/water separation. *J Membr Sci* 635:119502. <https://doi.org/10.1016/j.memsci.2021.119502>
- [13] Qiu L, Sun Y, Guo Z (2020) Designing novel superwetting surfaces for high-efficiency oil-water separation: design principles, opportunities, trends and challenges. *J Mater Chem A* 8:16831–16853. <https://doi.org/10.1039/D0TA02997A>
- [14] Wang Y, Yang H, Chen Z et al (2018) Recyclable oil-absorption foams via secondary phase separation. *ACS Sustain Chem Eng* 6:13834–13843. <https://doi.org/10.1021/acssuscchemeng.8b01950>
- [15] Qiu S, Li Y, Li G, Zhang Z, Li Y, Wu T (2019) Robust superhydrophobic sepiolite-coated polyurethane sponge for highly efficient and recyclable oil absorption. *ACS Sustain Chem Eng* 7:5560–5567. <https://doi.org/10.1021/acssuschemeng.9b00098>
- [16] Sakthivel T, Reid DL, Goldstein I, Hench L, Seal S (2013) Hydrophobic high surface area zeolites derived from fly ash for oil spill remediation. *Environ Sci Technol* 47:5843–5850. <https://doi.org/10.1021/es3048174>
- [17] Choi HM, Cloud RM (1992) Natural sorbents in oil spill cleanup. *Environ Sci Technol* 26:772–776. <https://doi.org/10.1021/es00028a016>
- [18] Tang Y, Zheng Q, Chen B, Ma Z, Gong S (2017) A new class of flexible nanogenerators consisting of porous aerogel films driven by mechanoradicals. *Nano Energy* 38:401–411. <https://doi.org/10.1016/j.nanoen.2017.06.022>
- [19] Zhao Y, Shen L, Yuan Y, Xiao L, Cai J, Lu Z, Hou L (2023) Preparation of porous poly(4-tert-butylstyrene) based monoliths with high efficiency for oil-water separation via high internal phase emulsion template. *J Appl Polym Sci* 140:e53801. <https://doi.org/10.1002/app.53801>
- [20] Liu T, Li D, Huang K, Tan S, Huang L (2023) Preparation and water/oil separation of super-hydrophobic biomass adsorbent based on three-dimensional graphene aerogel. *J Chem Technol Biotechnol* 98:744–755. <https://doi.org/10.1002/jctb.7279>
- [21] Ma W, Lu T, Cao W, Xiong R, Huang C (2023) Bioinspired nanofibrous aerogel with vertically aligned channels for efficient water purification and salt-rejecting solar desalination. *Adv Funct Mater* 2023:2214157. <https://doi.org/10.1002/adfm.202214157>
- [22] Yang Y, Chen X, Li Y, Yin Z, Bao M (2021) Construction of a superhydrophobic sodium alginate aerogel for efficient oil absorption and emulsion separation. *Langmuir* 37:882–893. <https://doi.org/10.1021/acs.langmuir.0c03229>
- [23] Zhuo L, Ma C, Xie F, Chen S, Lu Z (2020) Methylcellulose strengthened polyimide aerogels with excellent oil/water separation performance. *Cellulose* 27:7677–7689. <https://doi.org/10.1007/s10570-020-03311-6>
- [24] Lin B, Wang Z, Zhu Q, Binti Hamzah WN, Yao Z, Cao K (2020) Aerogels for the separation of asphalt-containing oil-water mixtures and the effect of asphalt stabilizer. *RSC Adv* 10:24840–24846. <https://doi.org/10.1039/D0RA00544D>
- [25] Ieamviteevanich P, Palaporn D, Chanlek N, Poo-arporn Y, Mongkolthananuk W, Eichhorn SJ, Pinitsoontorn S (2020) Carbon nanofiber aerogel/magnetic core-shell nanoparticle composites as recyclable oil sorbents. *ACS Appl Nano Mater* 3:3939–3950. <https://doi.org/10.1021/acsanm.0c00818>
- [26] Jiang J, Zhang Q, Zhan X, Chen F (2019) A multifunctional gelatin-based aerogel with superior pollutants adsorption, oil/water separation and photocatalytic properties. *Chem Eng J* 358:1539–1551. <https://doi.org/10.1016/j.cej.2018.10.144>
- [27] Bai X, Yuan Z, Lu C, Zhan H, Ge W, Li W, Liu Y (2023) Recent advances in superwetting materials for separation of oil/water mixtures. *Nanoscale* 15:5139–5157. <https://doi.org/10.1039/D2NR07088J>
- [28] Chhajed M, Verma C, Gupta P, Maji PK (2023) Multifunctional esterified nanocellulose aerogel: impact of fatty chain length on oil/water separation and thermal insulation. *Cellulose* 30:1717–1739. <https://doi.org/10.1007/s10570-022-04993-w>
- [29] Fox CH, Hurne GM, Wojtecki RJ et al (2015) Supramolecular motifs in dynamic covalent PEG-hemiaminal organogels. *Nat Commun* 6:7417. <https://doi.org/10.1038/ncomms8417>
- [30] Li Z, Qiu J, Yuan S, Luo Q, Pei C (2017) Rapidly degradable and sustainable polyhemiaminal aerogels for self-driven efficient separation of oil/water mixture. *Ind Eng Chem Res* 56:6508–6514. <https://doi.org/10.1021/acs.iecr.7b00312>
- [31] Guan X, Ma Y, Yang L et al (2020) Unprecedented toughening high-performance polyhexahydrotriazines constructed by incorporating point-face cation- $\pi$  interactions in

- covalently crosslinked networks and the visual detection of tensile strength. *Chem Commun* 56:1054–1057. <https://doi.org/10.1039/C9CC08603J>
- [32] Wang Y, Zhang L, Yang L, Chang G (2020) An indole-based smart aerogel for simultaneous visual detection and removal of trinitrotoluene in water via synergistic effect of dipole- $\pi$  and donor-acceptor interactions. *Chem Eng J* 384:123358. <https://doi.org/10.1016/j.cej.2019.123358>
- [33] Li Y, Du M, Yang L et al (2021) Hydrophilic domains compose of interlocking cation- $\pi$  blocks for constructing hard actuator with robustness and rapid humidity responsiveness. *Chem Eng J* 414:128820. <https://doi.org/10.1016/j.cej.2021.128820>
- [34] Wang Y, Liu D, Zheng Q et al (2014) Disulfide bond bridge insertion turns hydrophobic anticancer prodrugs into self-assembled nanomedicines. *Nano Lett* 14:5577–5583
- [35] Briggs D, Beamson G (1993) XPS studies of the oxygen 1s and 2s levels in a wide range of functional polymers. *Anal Chem* 65:1517–1523. <https://doi.org/10.1021/ac00059a006>
- [36] Cheng Y, Guan S, Li D, Zhu J, Zeng B (2019) Robust and durable superhydrophobic cotton fabrics via a one-step solvothermal method for efficient oil/water separation. *Cellulose* 26:2861–2872. <https://doi.org/10.1007/s10570-019-02267-6>
- [37] Meng X, Dong Y, Zhao Y, Liang L (2020) Preparation and modification of cellulose sponge and application of oil/water separation. *RSC Adv* 10:41713–41719. <https://doi.org/10.1039/D0RA07910C>
- [38] Jha P, Koiry SP, Sridevi C, Putta V, Gupta D, Chauhan AK (2020) A strategy towards the synthesis of superhydrophobic/superoleophilic non-fluorinated polypyrrole nanotubes for oil-water separation. *RSC Adv* 10:33747–33752. <https://doi.org/10.1039/D0RA06409B>
- [39] Li X, Zhang T, Xu Z, Chi H, Wu Z, Zhao Y (2020) Amphiphobic polyHIPEs with pH-triggered transition to hydrophilicity-oleophobicity for the controlled removal of water from oil-water mixtures. *Polym Chem* 11:6935–6943. <https://doi.org/10.1039/D0PY01144D>
- [40] Wang B, Yang X, Sha D, Shi K, Xu J, Ji X (2020) Silane functionalized polyvinyl-alcohol formaldehyde sponges on fast oil absorption. *ACS Appl Polym Mater* 2:5309–5317. <https://doi.org/10.1021/acsapm.0c01052>
- [41] Zhu C, Jiang W, Hu J, Sun P, Li A, Zhang Q (2020) Polylactic acid nonwoven fabric surface modified with stereo-complex crystals for recyclable use in oil/water separation. *ACS Appl Polym Mater* 2:2509–2516. <https://doi.org/10.1021/acsapm.9b01197>
- [42] Guo Z, Long B, Gao S et al (2021) Carbon nanofiber based superhydrophobic foam composite for high performance oil/water separation. *J Hazard Mater* 402:123838. <https://doi.org/10.1016/j.jhazmat.2020.123838>
- [43] Han L, Wu W, Huang Z et al (2021) Preparation and characterization of a novel fluorine-free and pH-sensitive hydrophobic porous diatomite ceramic as highly efficient sorbent for oil-water separation. *Sep Purif Technol* 254:117620. <https://doi.org/10.1016/j.seppur.2020.117620>
- [44] Chang G, Wang Y, Wang C, Li Y, Xu Y, Yang L (2018) A recyclable hydroxyl functionalized polyindole hydrogel for sodium hydroxide extraction via the synergistic effect of cation- $\pi$  interactions and hydrogen bonding. *Chem Commun* 54:9785–9788. <https://doi.org/10.1039/C8CC05819A>
- [45] He C, Huang J, Li S, Meng K, Zhang L, Chen Z, Lai Y (2018) Mechanically resistant and sustainable cellulose-based composite aerogels with excellent flame retardant, sound-absorption, and superantwettable ability for advanced engineering materials. *ACS Sustain Chem Eng* 6:927–936. <https://doi.org/10.1021/acssuschemeng.7b03281>
- [46] Zhu T, Cheng Y, Huang J et al (2020) A transparent superhydrophobic coating with mechanochemical robustness for anti-icing, photocatalysis and self-cleaning. *Chem Eng J* 399:125746. <https://doi.org/10.1016/j.cej.2020.125746>
- [47] Li J, Yang L, Liu H, Li G, Li R, Cao Y, Zeng H (2020) Simple preparation method for hydrophilic/oleophobic coatings. *ACS Appl Mater Interfaces* 12:45266–45273. <https://doi.org/10.1021/acsami.0c11596>
- [48] Bai X, Shen Y, Tian H, Yang Y, Feng H, Li J (2019) Facile fabrication of superhydrophobic wood slice for effective water-in-oil emulsion separation. *Sep Purif Technol* 210:402–408. <https://doi.org/10.1016/j.seppur.2018.08.010>

**Publisher's Note** Springer Nature remains neutral with regard to jurisdictional claims in published maps and institutional affiliations.

Springer Nature or its licensor (e.g. a society or other partner) holds exclusive rights to this article under a publishing agreement with the author(s) or other rightsholder(s); author self-archiving of the accepted manuscript version of this article is solely governed by the terms of such publishing agreement and applicable law.